ARMA 24–0760

A Study of the Key Factors Associated with a Massive Pillar Failure in an Underground Limestone Mine using Numerical Models

Rashed, G., Yuting X., and Evanek N.

NIOSH Pittsburgh Mining Research Division, Pittsburgh, PA, USA

ABSTRACT: Several massive ground collapses occurred in the past decade in US underground stone mines where surface subsidence occurred in most of them. The occurrence of a massive ground collapse in stone mines places the mine workers at great risk. The National Institute for Occupational Safety and Health (NIOSH) initiated a project to better understand the causes of these massive collapses and reduce/eliminate their future occurrence. Previously the authors investigated one of these massive collapses and it was found that pillar failure was the most likely cause for the collapse. In this study, the authors further investigated the impact of pillar benching, karst cavities, and geological discontinuities on the potential for pillar failure. 3D LiDAR scans were utilized to determine the extent, location, and dimensions of the karst cavities. Stress and deformation analysis were conducted using 3DEC models to gain more insight about the impact of floor benching and poor rock mass quality on stone pillar stability. Poor rock mass quality can be attributed to the existence of karst cavities, small joint spacing, and poor joint conditions at the study mine. Based on the numerical modeling results, floor benching in association with linear karst cavity and geological discontinuities in pillars can create a large uncontrolled displacement, sliding along pre-existing joints, and induce tensile stresses near the center of the pillar that may result in a brittle pillar failure.

INTRODUCTION

Between 2015 and 2021, five massive ground collapses occurred in underground room-and-pillar stone mines in the United States (Evanek et al., 2022 and Rumbaugh et al., 2022). The depth of cover at these collapses was less than 600 ft (~183 m). These events pose a significant risk of ground failure and air blast that may result in injuries, fatalities, destruction of ventilation controls, and a potential surface subsidence (Evanek et al., 2022). In general, massive collapses can be attributed to roof or pillar failure. An example of massive roof failure is the collapse that occurred at the Lake Lynn Experimental Mine (Iannacchione et al. 2007), while the collapse that occurred at Whitney mine was an example of pillar failure (Esterhuizen et al., 2018).

In 2020, a massive collapse occurred in an underground limestone mine in southwestern Pennsylvania. Shortly after the massive collapse had occurred, researchers from the National Institute for Occupational Safety and Health (NIOSH) conducted 3D LiDAR scans nearby the collapsed area. Accurate mine geometries as well as geological anomalies were extracted from these scans. The collapse occurred only in a benched area in the mine where the mine extracts the Loyalhanna formation. The depth of cover at the collapsed area is about 170 ft (51.8 m) and the average extraction ratio is about 81%. The as-designed pillar size was about 40 x 40 ft (12.1 x 12.1 m), while on average, the as-mined pillar size around the collapsed area estimated from LiDAR scans was about 35 x 35 ft (10.6 x 10.6 m) with a few pillars as low as 27-ft (8.2-m) wide.

Rashed et al. (2023) investigated that collapse to answer two questions: First, was the collapse initiated by pillar failure or roof failure? Second, if it was a roof or pillar failure, why did it fail? It was concluded that the massive collapse at that mine was triggered by pillar failure based on the following: 16 Unconfined Compressive Strength (UCS) tests and 34-point load tests were conducted from samples around the collapsed area, borescope data at four different locations nearby the collapsed area, 3D LiDAR scans for both the sink hole over the collapse and the underground mine workings, field observations, and numerical models. The occurrence of pillar failure was attributed to low rock mass quality, due to karst cavities and geological discontinuities, and a small width-to-height (w/h) ratio of some pillars because of the floor benching.

This study is a follow-up to what Rashed et al. (2023) previously completed. The main objective of this work is to utilize numerical models to investigate the impact of floor benching, geological discontinuities, and karst cavities (the study parameters) on stone pillar stability. More emphasis was placed on the load change and stress transfer that occurred because of floor benching. Additionally, a focus in the study was how floor benching in association with geological discontinuities can trigger shear failure along pre-existing joints and reduce the confining stress in pillars. Floor benching, geological discontinuities, and karst cavities can combine/interact to create potential problems in underground stone mines that might lead to brittle failure. The impact of each one of these parameters on pillar stability will be explored and linked to the study mine in the sections that follow.

FLOOR BENCHING IN UNDERGROUND STONE MINES

Floor benching is common in underground stone mines, and it is carried out to better utilize the reserve and maximize the profit. During a previous study at NIOSH, out of 31 visited mines, 18 of them practiced bench mining of the floor (Esterhuizen et al., 2007). Figure 1 shows an area where floor benching was conducted in an underground stone mine.

Mining the floor increases the pillar height which creates slender pillars. The strength and stiffness of slender (fully benched) pillars are less than wider (development) pillars of the same cross-sectional area due to the reduction in the w/h ratio of the pillar (Rumbaugh et al., 2022). The reduction in pillar strength can be estimated using the S-Pillar or any other empirical pillar strength equation for hard rock mine (Hoek, et al., 1995; Martin and Maybee, 2000; Esterhuizen et al., 2011).

Slender pillars may behave differently from wider pillars because of the absence of a confined core. Slender pillars can be weaker than predicted from models since they are more sensitive to local geological discontinuities (Esterhuizen et al., 2008).

Figure 1: Development pillar height versus benched pillar height in an underground limestone mine.

Floor benching increases the load on perimeter pillars that are not benched yet and reduces frictional resistance along planes of weakness in benched pillars. These points will be explained in detail later in the paper. Esterhuizen et al. (2007) observed evidence of increased instability of pillars at the perimeter of the benched areas. The instability was in the form of failure along the pre-existing geological structure and stress-related spalling and fracturing of the pillar ribs.

The massive collapse that has been modeled/investigated in this study occurred only in benched areas with most of the collapse occurring in the full bench area with a pillar height of 48 ft (14.6 m). The collapse did not propagate to the unbenched areas where the pillar height is 26 ft (~8 m). The collapse encompassed a 5x6 array of pillars; see Figure 2 which shows the collapse periphery (red box) at the study mine. Some pillars in the collapsed area have a w/h ratio <0.8 which is not recommended by the S-Pillar guidelines for stone pillar design (Esterhuizen, et al., 2011).

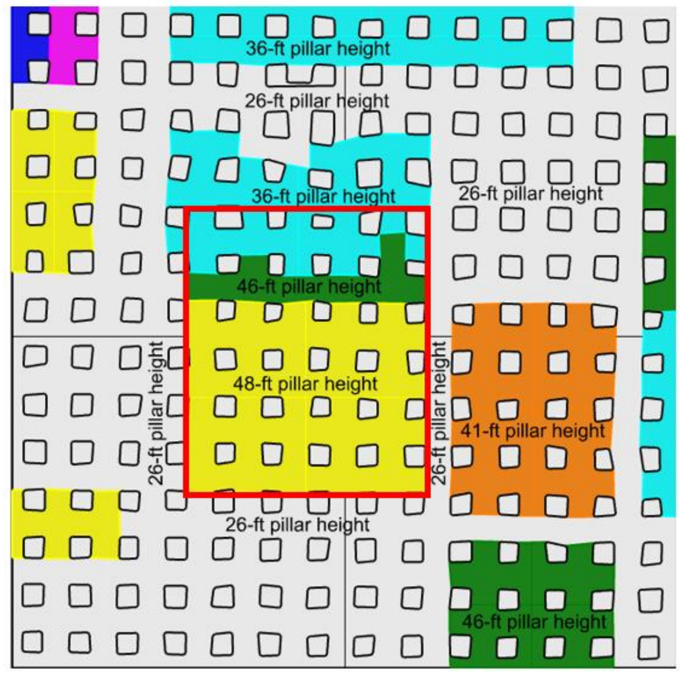

Figure 2: Massive ground collapse periphery is surrounded by a red box; different colors reflect different floor benching height. The maximum pillar height is 48 ft (14.6 m) after floor benching.

ANISOTROPY IN UNDERGROUND LIMESTONE MINES

Usually, the behavior of stone pillars in underground mines is anisotropic due to the presence of geological discontinuities, such as joints and bedding planes. The importance of these features stems from the fact that rock mass becomes weaker, more deformable, and highly anisotropic because there is reduced shear strength and higher permeability parallel to discontinuities and reduced tensile strength perpendicular to them (Goodman, 1989).

When a rock mass is excavated, some joints will close up while others will open, and some blocks will slide against each other along joint surfaces. The frictional strength of interlocking rock surfaces is governed by Coulomb's shear strength criterion. The majority of unweathered rock surfaces have values of the basic friction angle ranging from 25° to 35°, at least at medium stress levels. The peak friction angle of unfilled rock joints at low normal stress (< 0.5 MPa) can reach 80° (Barton, 1976).

Bandis et al. (1983) found that as the scale/length of the sheared surface increases, the effective roughness of the surface decreases and hence the shear strength of the surface decreases. The apparent friction angle and the roughness angle decrease with increasing scale. Hence, the role of the basic friction angle would dominate the shear strength of the surface. Jaeger (1960) found that the orientation of the critical plane at which the shear strength will be reached first is ($45^{\circ} + \phi/2$). Hence, for a friction angle between 30º–40º, the orientation of the critical plane would be between 60º and 65º.

At the study mine, the geological discontinuities nearby the collapse region were mapped, and two steeply dipping joint sets were identified, J1 and J2. The dip of the joint sets ranges from around 75º to 90º. J1 was more prominent than J2 with joint spacing ranges from about 5 to 12 ft (1.5 to 3.6 m), and some pillars around the collapse have four joints dipping around 75º. Very few bedding discontinuities were observed and did not appear to affect pillar integrity.

Some joints around the collapsed area were iron stained, especially in the dominant joint set (J1). Figure 3 shows two near-vertical, large iron-stained joints in a pillar on the southwestern side of the collapsed area. Iron staining in joints indicates open apertures that easily transmit water and offer little to no cohesion between opposing blocks of rock (Phillipson, 2012). Details of the mining and geological conditions are presented in Rashed et al. (2023).

Figure 3: Two near-vertical, large iron-stained joints in a pillar nearby the collapsed area.

KARST CAVITIES OBSERVED NEARBY THE COLLAPSED AREA

Carbonate rocks, such as dolomites and limestones are susceptible to solution by slightly acid waters percolating initially through discontinuities in the rock mass. With time, volumes of rock can be dissolved leading to what are known as karst features/cavities (Brady and Brown, 2004).

Karst cavities may present ground-control risks and hazards, and in addition to being pre-existing structural discontinuities, they act as conduits for water flow in the rock mass (Baggett et al., 2020). Additionally, they weaken the pillar since the limestone material was removed and this creates a void. Furthermore, stresses (tension and compression) tend to be high at the boundary of the karst cavity.

Karst cavities of various sizes with an elliptical shape were observed in the area nearby the collapsed region in the study mine, Figure 4 shows two examples for karst cavities of different sizes. The width of the cavity shown in Figure 4b is about 2.5 ft (0.8 m), and it decreases in size toward the pillar core; the height of that cavity is about 9.5 ft (2.9 m), and its depth is about 17 ft (5.2 m) deep inside the pillar, determined from the LiDAR scan. The scanner may not have captured the full extent of the karst cavity into the pillars. On the other hand, the dimension of the cavity shown in Figure 4a is relatively small compared to Figure 4b.

The extent/depth of the karst cavities into three pillars on the northeastern side of the collapsed area from the 3D LiDAR scan is shown in Figure 5. Measurement of the largest extent captured for karst cavities is approximately 21 ft (6.4 m).

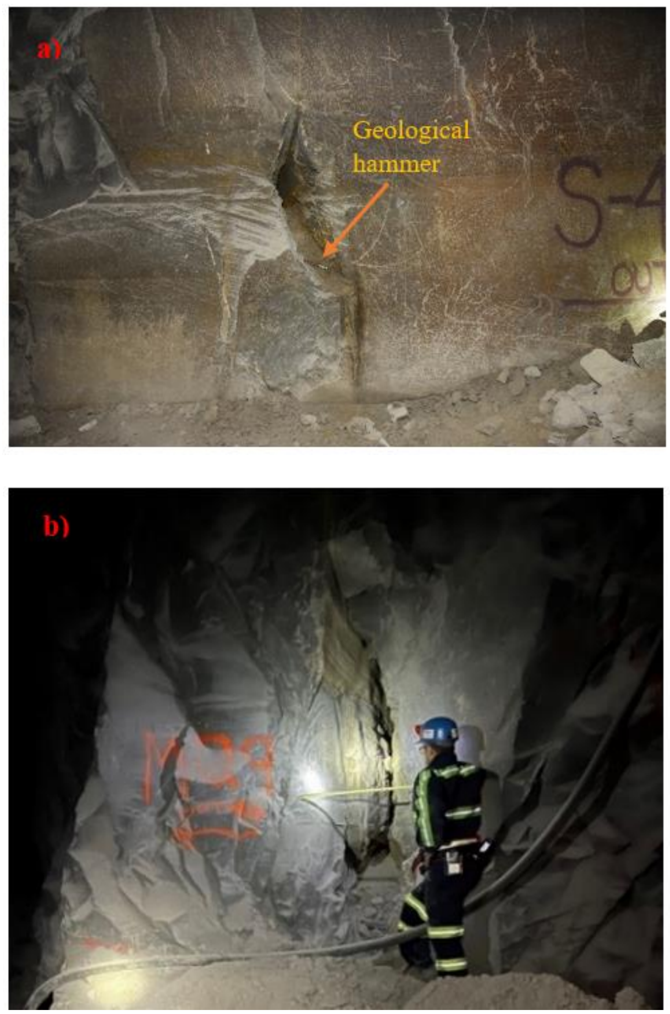

Figure 4: Karst cavities of different sizes observed nearby the collapsed area in the study mine: a) small size and b) large size.

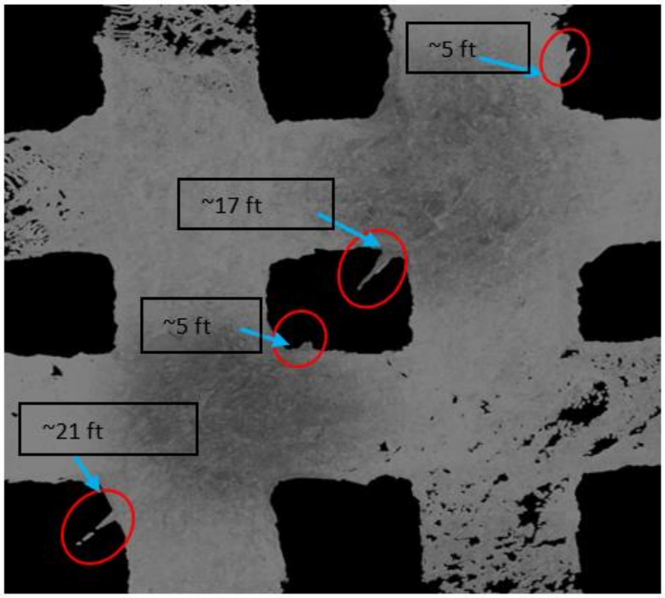

Figure 5: 3D LiDAR image of the large linear karst feature extending into multiple pillars on the northeast side of the massive ground collapse.

MODEL SETUP FOR THE STUDY MINE

In this study, numerical models were utilized to gain more understanding about pillar stability in response to bench mining activities with and without geological discontinuities and karst cavities. Large-scale 3DEC models (Itasca, 2019) were generated to investigate the role of these parameters in the massive collapse that occurred in the study mine.

To generate a 3D large-scale model, the 2D mine map was exported to Rhinoceros software to generate a 3D mine geometry and surface mesh (McNeel et al., 2010); then Griddle software was used to generate a volume mesh ready to be exported to 3DEC software to conduct stress/deformation analysis (Itasca, 2020). A plan view for a 3DEC model at the mine level is shown in Figure 6.

Various scenarios were modeled to simulate various combinations of the study parameters including and not limited to the following scenarios: Scenario one, it was presumed that all modeled pillars are massive and free from joints; Scenario two, a pillar was selected in the massive collapsed area and made to be intersected by four parallel joints dipping at 75° with 6.5 ft (2.0 m) of joint-spacing (see Figure 6). This jointed pillar is referred to as the study pillar. The study pillar was selected due to the location of the pillar along the projection of the largest linear karst feature (Figure 5). The joint dip and spacing reflect the conditions observed around the massive collapsed area; Scenario three, the study pillar has a linear karst cavity near mid-height of the pillar after benching. Scenario four, which models the most adverse conditions that could apply to this site and includes both a large linear karst feature and four parallel joints dipping at 75° with 6.5 ft (2.0 m) of joint-spacing.

In this study, an elastic material model was used for pillars and the rock mass around them. The authors believe that there is no need to use nonlinear material models because the dominant mode of failure would be gravity-driven sliding on discontinuities that exist in the study pillar. Stress-induced failure of intact rock material is expected to be minimal and plays a minor role in the behavior of the rock mass failure because the in-situ stresses are low, the depth of cover is around 170 ft (51.8 m) at the collapsed site. Additionally, the use of elastic models in this study can also be justified with the findings by Hoek and Brown (1980), they found that the rock mass response is elastic if the ratio (σ_1/σ_{ci}) < 0.15, where σ_1 is the major far field in situ principal stress and σ_{ci} is the intact rock strength. This ratio is satisfied at the study mine.

The in-situ rock mass modulus was estimated from Hoek and Diederichs (2006) assuming a geological strength index of 75 for the rock mass. Explicit interfaces were used to simulate bedding planes at the roof/floor lines, also joints may or may not exist in the study pillar depending on the modeled scenario. 3DEC provides interfaces that are characterized by Coulomb sliding and/or tensile and shear bonding (Itasca, 2019). The mechanical properties that were used to simulate the limestone rock mass and geological discontinuities are summarized in Table 1. There are no signs of high horizontal stresses in the mine, which is why the horizontal to vertical stress ratio was assumed to be 0.5.

3DEC models were solved in four stages: (1) Geostatic stage, in which the pre-mining in-situ stresses are initialized; (2) Development stage, in which all headings and crosscuts were excavated. (3) Development of the karst cavity, if the modeling scenario includes karst cavity in the study pillar. (4) Floor benching with cutting sequence conducted on 6 stages. The element size for pillars in the full bench area was constant and equal to 1.6 ft (0.5 m) in all models.

Table 1: Interface properties used in 3DEC model to simulate the joint conditions in the study pillar.

Parameter	**Value**
Intact Young's Modulus ($\boldsymbol{E_i}$), (GPa)	50E6
Poisson's ratio (ν)	0.25
Normal stiffness (kn), MPa/m	15,000
Shear stiffness (ks), MPa/m	5,000
Friction angle (φ), degree	30.0
Dilation angle (Ψ), degree	15.0
Cohesion (c), MPa	1.0
Tension (σ_t), MPa	0.5

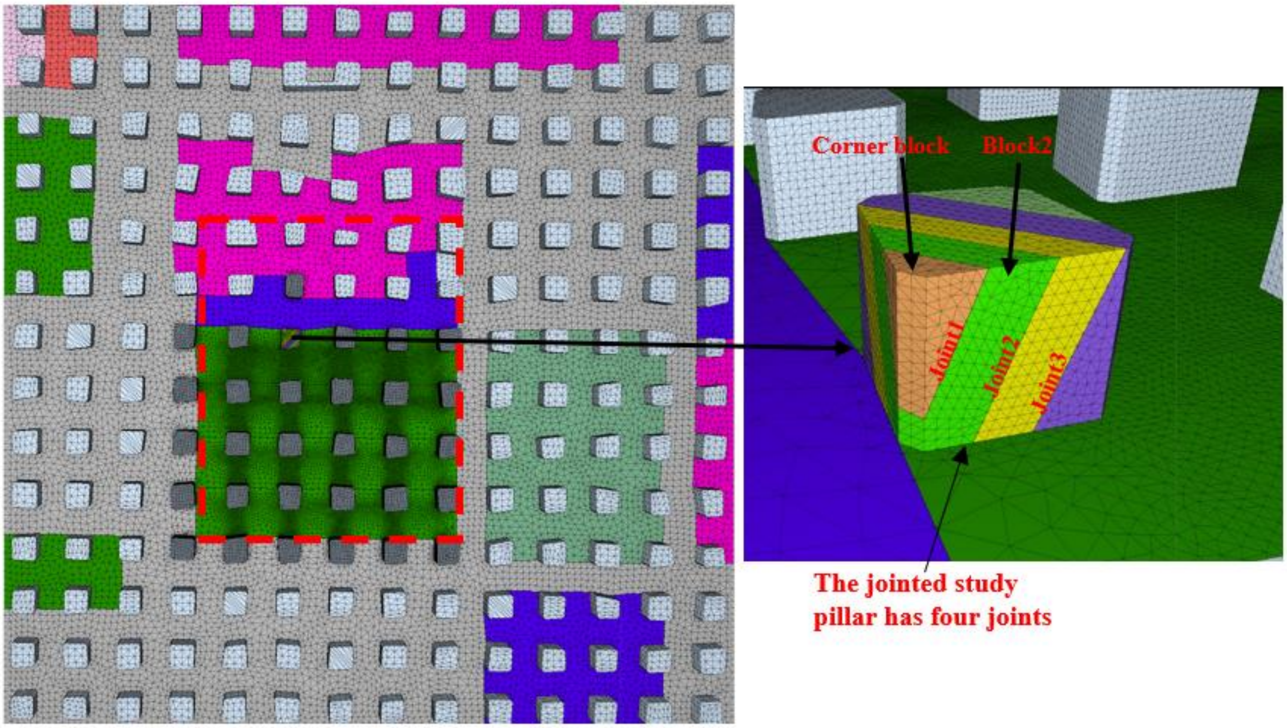

Figure 6: A plan view for a large-scale 3DEC model at the mine level with zoom-in at a jointed study pillar. The dotted red box contains the collapsed area.

NUMERICAL ANALYSIS FOR THE EFFECT OF BENCHING ON THE STABILITY OF A MASSIVE STONE PILLAR

3DEC models were used to evaluate changes in pillar loading and likely stress transfer during floor bench mining. In this section, the modeled pillars are presumed massive, such that joints and bedding planes do not exist. Figure 7 shows a 3DEC model in which the initial developed pillars, the perimeter pillars, and the fully benched pillars can be seen. Development pillars that have not been benched at the edge of the benched area are referred to as perimeter pillars. Fully benched pillars are those pillars with the floor being removed from all sides, while partly benched pillars are those pillars with the floor not removed from at least one side. Please note that the initial development pillars are significantly far from the benched area.

The model results for the maximum principal stress distribution at the development stage and during bench mining are presented in Figure 8. In the development stage, the stress distribution was even and symmetric across the pillars; see Figure 8a. Some pillars are more stressed than others probably because of their smaller cross-sectional area and slightly bigger room sizes around them. Floor benching creates an uneven/asymmetric stress distribution in partly benched and perimeter pillars at the edges of the benched area, such that one side of the pillar is highly stressed compared to the other side; see Figure 8b. In general, the perimeter pillars are subjected to an increase in average pillar stress. However, the partly and fully benched pillars experienced stress relaxation. The reduction in average pillar stress for fully benched pillars can be attributed to the reduction in their stiffness due to the increase in pillar height, causing the load to be transferred to the stiffer nearby pillars. Also, for the partly benched pillar, the short side of the pillar is stressed more than the tall side of the pillar because of the reduction in stiffness for the tall side.

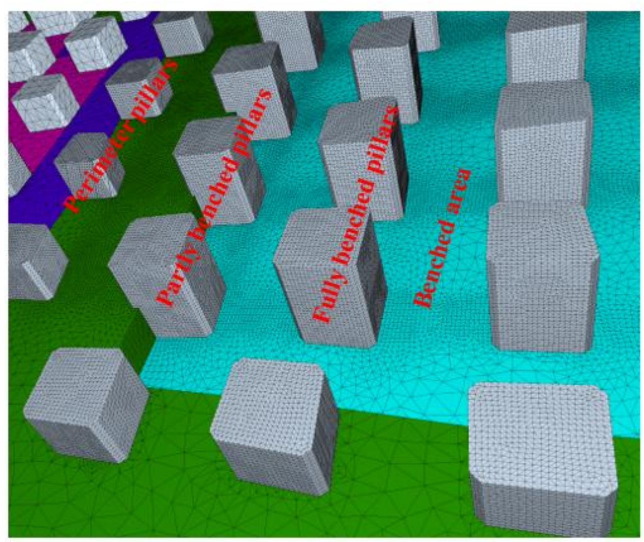

Figure 7: 3DEC model illustrating fully benched, partly benched, and perimeter pillars in the study mine.

Based on the model results, because of floor benching, the perimeter pillars are subjected to an increase of about 8% in their average stress with high local stresses near corners and sidewalls. These local stresses can initiate spalling and fractures in perimeter pillars. It is believed that many factors control how much load will transfer to the perimeter pillars during bench mining, including the bench height, the distance between the perimeter pillars and the face of the floor that is being benched, the depth of cover, and the benched area. Esterhuizen et al. (2007) observed that a number of pillars experienced progressive spalling to form an hourglass shape at the perimeter of a benched area. They also observed open vertical fractures and large slabs lying on the mine floor around these pillars. Pillar loading and stress transfer in response to floor benching is affected by the existence of discontinuities and karst cavities in the pillar.

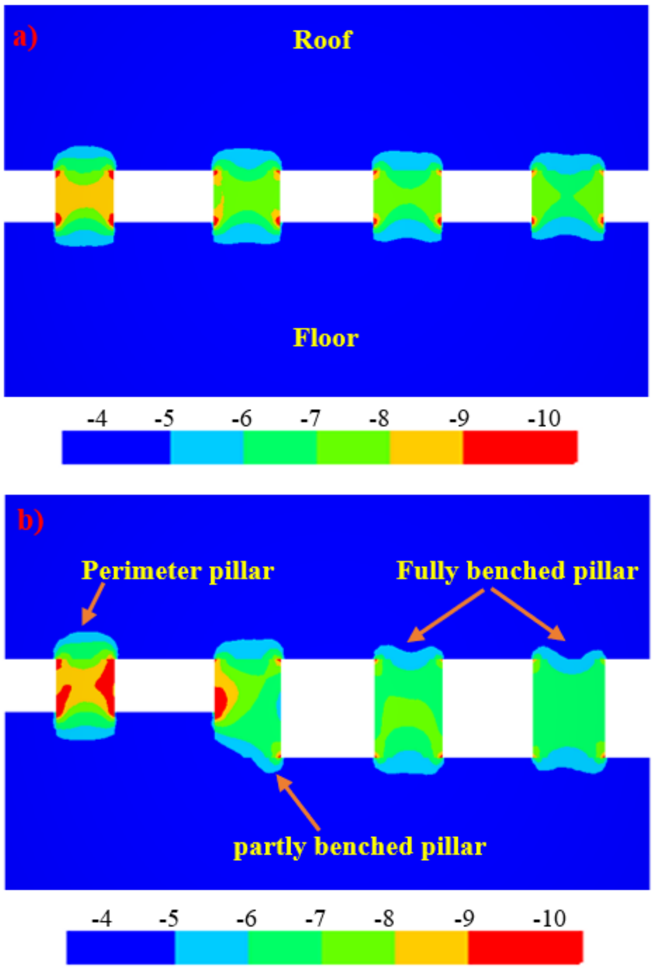

Figure 8: The maximum principal stress distribution at a) development loading stage and b) floor bench mining. Stress magnitudes are in MPa; negative values mean compression.

The confining stress in unbenched pillars is relatively large, and it increases with increasing the w/h ratio of the pillar. Floor benching affects the horizontal or confining stress distribution in pillars (see Figure 9). The minimum principal stress reduces at the center of fully benched pillars to become almost zero, and the minimum principal stress changed from compression to tension at the tall side of partly benched pillars. Tensile stresses could create tensile failure such that pre-existing cracks will propagate and open further while new cracks would develop. The existence of geological discontinuities in pillars would exacerbate the impact of floor benching on stone pillar stability. The combined effect of floor benching and geological discontinuities can trigger sliding along pre-existing joints and induce tensile stresses at the center of jointed pillars. These points will be explained in the next section.

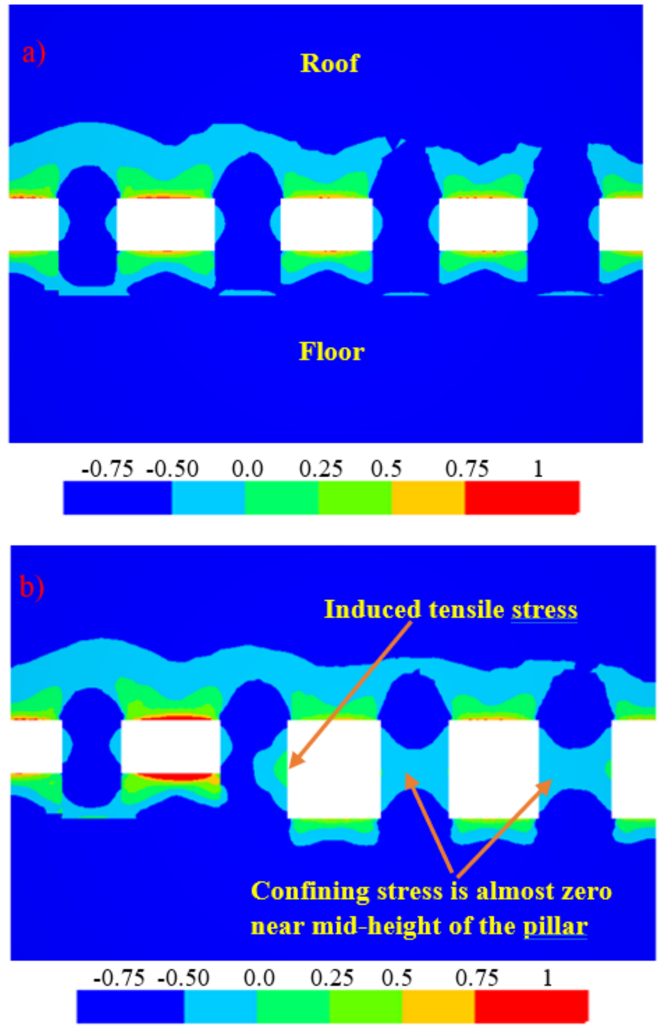

Figure 9: The minimum principal stress distribution at a) development loading and b) floor bench mining. Stress magnitudes are in MPa, and positive values mean tension.

FLOOR BENCHING CAN TRIGGER SLIDING ALONG PRE-EXISTING PLANES OF WEAKNESS

At shallow depths, structurally controlled failures may be the prime concern in excavation design (Brady and Brown, 2004). Slipping along pre-existing planes of weakness occurs if the driving shear force is greater than the resisting force. Floor benching may trigger a slip along one or more pre-existing joints by converting the joint from being constrained to being unconstrained. Figure 10 shows a schematic for both constrained and unconstrained joints. Constrained joints receive supplemental resistance and friction at both ends of the joints. After development, Joint2 shown in Figure 10 was constrained before floor benching where the floor was acting like a retaining wall that prohibit/minimize sliding along joint2. Once the floor was removed, joint2 became an unconstrained joint and its potential for sliding increased.

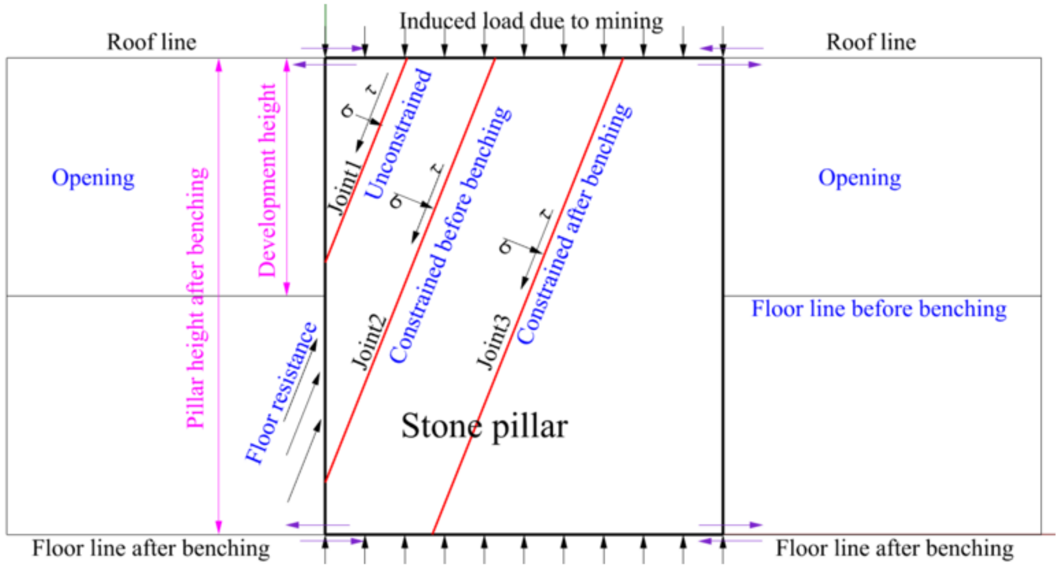

Figure 10: Schematic for constrained and unconstrained joints in an underground stone pillar.

In the previous section, the study pillar was presumed massive which is not the case in most underground stone mines. In this section, the study pillar is jointed (and has four joints) to gain more insight about the combined effect of floor benching and geological discontinuities on pillar stability (see Figure 6). Two of the four joints in the study pillar are constrained joints, while the other two are similar to joint1 and joint2 shown in Figure 10.

There is a lack of knowledge about the frictional resistance for joints in the study mine. Values for the internal friction angle have been reported by many authors in the literature, and a reasonable value appears to be 30º with most values in the range 21º–40º (Goodman, 1989). Also, Boyd (1975) found that most rock types have a basic friction angle of 30º.

In this study, the internal friction angle and cohesion for all joints in the study pillar are presumed 30º and 145 psi (1 MPa), respectively. Based on 3DEC model results, when the rock mass was excavated in the development stage, shear failure occurred along joint1, and the corner block was detached from the roof and slides toward the opening. The shear strength of joint1 was not high enough to hold the corner block in place.

Figure 11 shows the displacement magnitude for some pillars including the study pillar in the development stage. The displacement magnitude for the corner block of the study pillar was significantly high compared to other pillars. The shear displacement along joint1 was also high indicating shear failure. Both the displacement magnitude and joint shear displacement increased further with floor benching activities. The corner block was removed from the 3DEC model once its displacement magnitude reached about 60 mm. On the other hand, sliding along the other three constrained joints in the study pillar was prevented because of the floor resistance and friction generated at the ends of the joints.

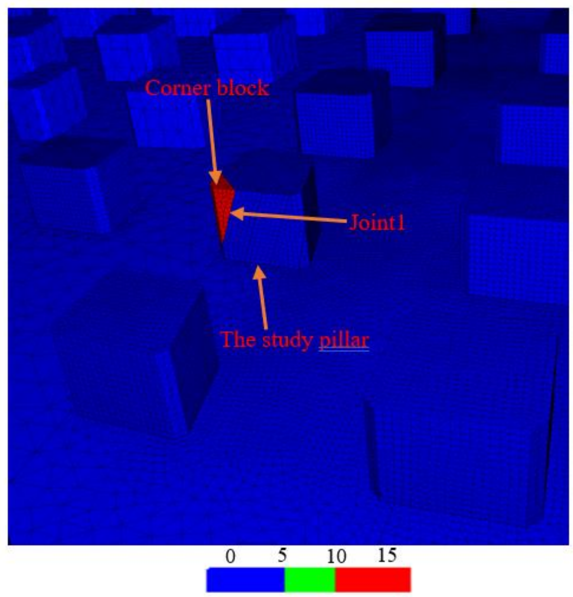

Figure 11: Displacement magnitude in mm for the development stage; the corner block of the jointed study pillar was removed from the model when its displacement reached 60 mm during benching.

In general, the sense of slip involves a differential displacement between the upper and lower surfaces of the joint which was prohibited for constrained joints. The maximum shear displacement on any of these joints was less than 0.3 mm and the normal joint displacement (joint dilation/opening) was almost zero. The numerical model results indicate that the strength of discontinuities which were free to dilate was much lower than the strength of those which were constrained.

Floor benching triggered a large and uncontrolled displacement of block2 associated with sliding along joint2 (see Figure 12). Block2 was also removed from the 3DEC model after its displacement magnitude reached 40 mm. The removal of the corner block and block2 from the model —physically means that the block failed and laid on the floor— resulted in an increase in the average pillar stress of the study pillar and the nearby pillars.

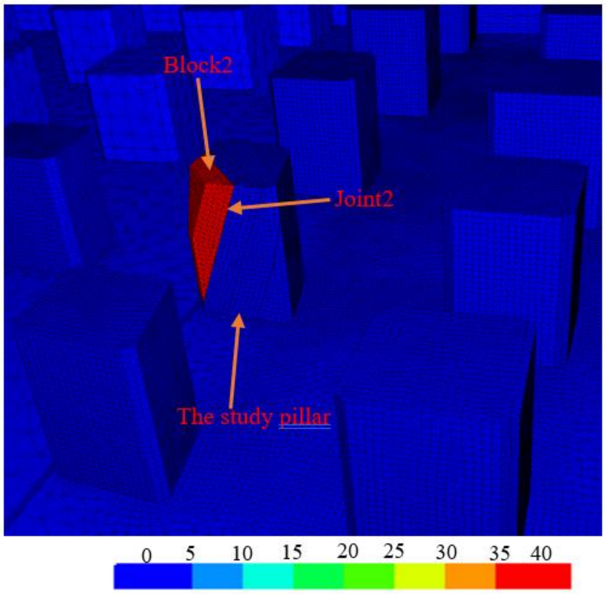

Figure 12: Displacement magnitude in mm; floor benching triggered sliding along joint2.

Floor benching may create unfavorable conditions that could place fully benched jointed pillars at risk of brittle failure. Floor benching significantly released the confining stresses within the jointed pillar and could create tensile stresses around the center of the pillar. See Figure 13 that shows the minimum principal stress distribution across four pillars in the collapsed area including the study pillar. The center and sidewalls of the study pillar are subjected to vertical compression and horizontal tension; this loading condition will increase the joint dilation that tends to loosen/weaken the rock mass and with time can lead to a brittle failure.

Floor benching can also reduce the normal stress on joint planes of fully benched pillars. For example, by comparing the normal stress on joint2 in the study pillar before and after benching, it was found that the normal stress reduced by 94% when the jointed study pillar was fully benched. That means the shear strength of joint2 became mainly cohesive since its frictional resistance was almost zero because of the substantial reduction in the normal stress.

It is important to mention that floor benching triggered sliding along joint2 because the shear strength of that joint was not high enough to prevent the shear failure. The authors found in using 3DEC models that shear failure will not occur if the joint cohesion increased from 145 psi (1 MPa) to 290 psi (2 MPa) while the friction angle stays the same at 30º. An analytical solution using Coulomb's shear strength criterion shows that the safety factor for shear failure was more than 1.0 when the joint cohesion increased to 290 psi (2 MPa).

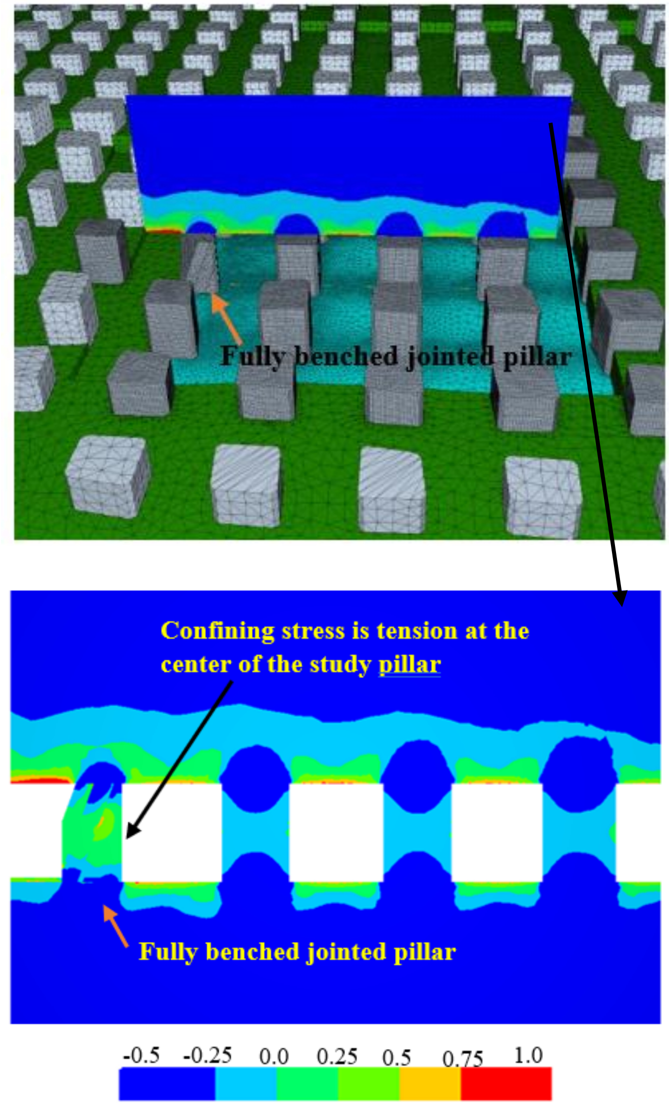

Figure 13: 3DEC model and the minimum principal stress distribution in MPa at a cross-section through four pillars including the study pillar in the collapsed area.

During floor benching activities, pillars are subjected to a cycle of "loading-unloading-reloading." Figure 14 shows the average vertical stress in the study pillar from the development stage to the fully benched stage. The average vertical stress in the study pillar was calculated 13 ft from the roofline. After development, the loading cycle started with floor benching such that the average vertical stress increased in the pillar for being a perimeter pillar. The unloading cycle occurred when the pillar became partly benched and the stress relaxation increased further when the pillar was fully benched. As floor benching continues and the benched area increases, the stress in the fully benched pillars is expected to gradually increase back to the tributary stress, "reloading" again. This loading cycle is shown in Figure 14. The average stress in the pillar increases further when some blocks from the pillar slide and fail. This cycle of "loading-unloading-reloading" might cause failure and initiate cracks in the sidewalls of fully benched pillars.

During floor benching activities, pillars are subjected to a cycle of "loading-unloading-reloading." Figure 14 shows the average vertical stress in the study pillar from the development stage to the fully benched stage. The average vertical stress in the study pillar was calculated 13 ft from the roofline. After development, the loading cycle started with floor benching such that the average vertical stress increased in the pillar for being a perimeter pillar. The unloading cycle occurred when the pillar became partly benched and the stress relaxation increased further when the pillar was fully benched. As floor benching continues and the benched area increases, the stress in the fully benched pillars is expected to gradually increase back to the tributary stress, "reloading" again. This loading cycle is shown in Figure 14. The average stress in the pillar increases further when some blocks from the pillar slide and fail. This cycle of "loading-unloading-reloading" might cause failure and initiate cracks in the sidewalls of fully benched pillars.

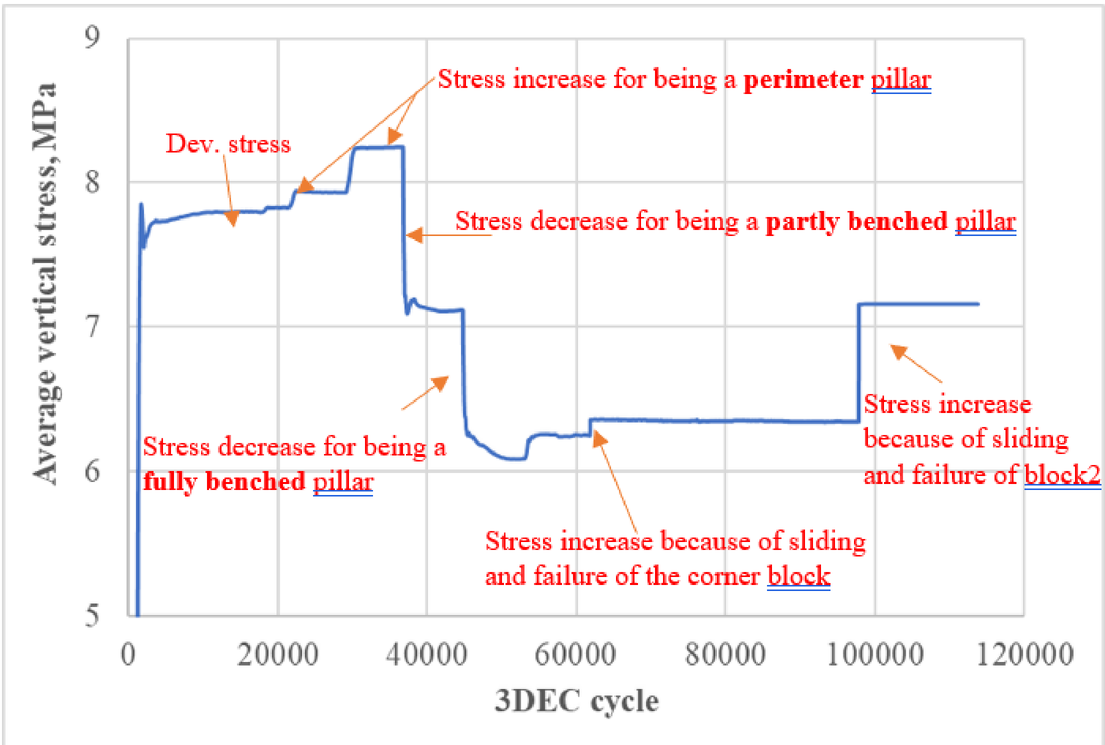

Figure 14: Loading cycle for an underground pillar from being a development pillar to become a fully benched pillar from a 3DEC model.

KARST CAVITIES COULD PRESENT GROUND-CONTROL RISK AND HAZARD

3DEC models were utilized to investigate the impact of karst cavity observed in the study mine on stone pillar stability during floor benching. The shape, dimensions, and orientation of the cavity used in the 3DEC models were taken from Figure 4b. However, the worst-case scenario was assumed such that the cross-sectional area of the cavity is constant, and it does not get smaller with depth inside the pillar. The karst cavity is located at mid-height of the study pillar after benching. Based on the 3DEC model results, the existence of karst cavity in a massive pillar did not induce any tensile stresses on the boundary of the cavity in the development stage. However, when the pillar was fully benched, tensile stresses occurred on the boundary of the cavity near the roof. The existence of geological discontinuities along with the cavity intensified the induced tensile stresses in the pillar. See Figure 15 that shows the minimum principal stress distribution in a karst pillar with and without joints. The combined effect of floor benching in association with karst cavity and jointing can create opening of joints because of the induced tensile stresses and accelerate weathering. Also the tangential stresses increase near the sidewalls of the cavity. Since a basic mining goal is to ensure that uncontrolled displacement of rock blocks in the excavation boundary will not occur, it is recommended to consult a geotechnical engineer before conducting floor benching in stone mines if the quality of the rock mass is poor. Joint conditions dominate the quality of rock mass. Joint conditions can change over time due to weathering or water drainage which could impact the shear strength of the joint. Weathering causes a reduction in rock properties such as the coefficient of friction of a surface. Hence, it is important to monitor changes in rock mass quality over time especially in fully benched areas. Phillipson (2023) reported that fully benched, 90-foot-tall pillars in the Galena Group of northern Illinois did not exhibit any sign of destress because the rock mass quality was very good with GSI 85. Phillipson (2023) also noted that the underground limestone mines that experienced massive collapses have GSI values ranging between 55 and 70.

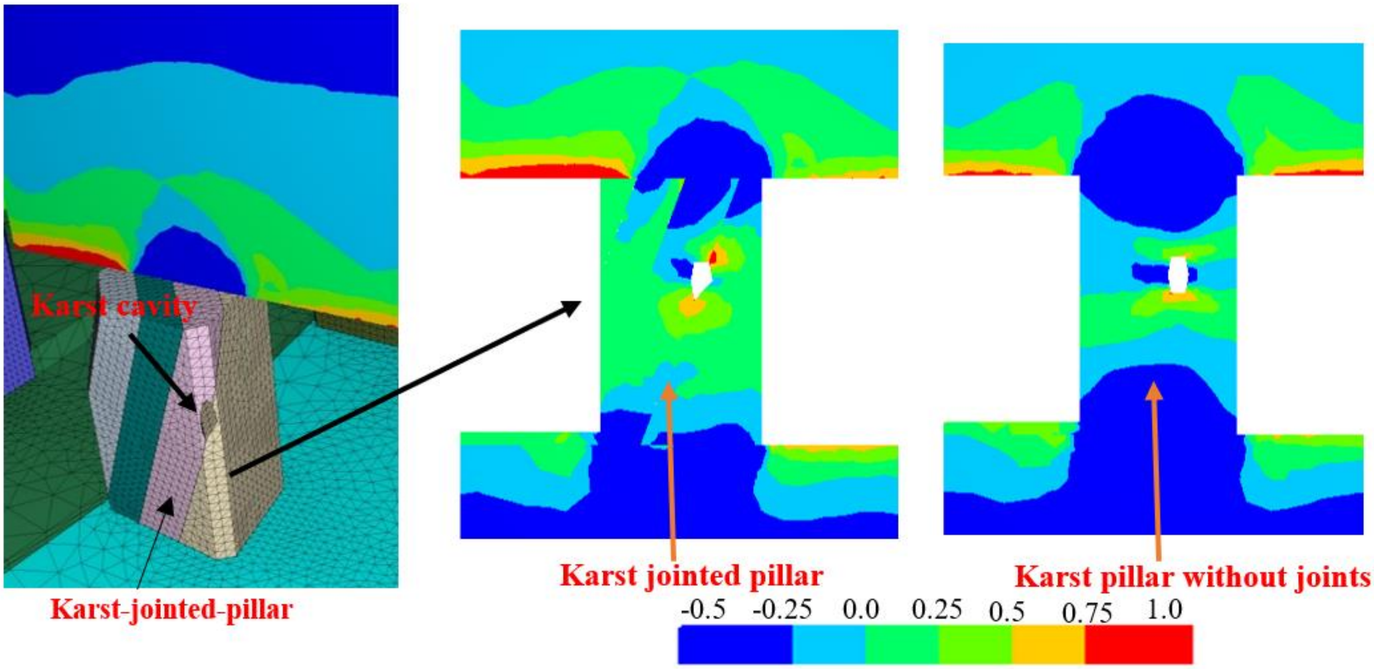

Figure 15: The minimum principal stress distribution for a karst, full benched pillar with and without joints from 3DEC models. Stress magnitudes are in MPa. Negative values mean compression.

SUMMARY AND CONCLUSION

In 2020, a massive collapse occurred in an underground limestone mine in southwestern Pennsylvania. Previously, NIOSH investigated that collapse and the evidence gathered strongly suggest that the massive collapse was triggered by pillar failure. The occurrence of pillar failure was attributed to a small w/h ratio of some pillars due to floor benching and low rock mass quality because of karst cavities and geological discontinuities. This study is a follow-up to what NIOSH previously completed and the main objective is to utilize numerical models to investigate the impact of floor benching, geological discontinuities, and karst cavities on pillar stability at the study site.

The study found that floor benching in association with geological discontinuities and karst cavities can create unfavorable conditions that could lead to brittle pillar failure. Floor benching creates asymmetric stress distribution in perimeter and partly benched pillars, such that one side of the pillar is highly stressed compared to the other side. Floor benching in association with geological discontinuities can induce tensile stresses at the center of the pillar and increase the joint dilation/opening. Joint dilation tends to loosen/weaken the rock mass. Floor benching also resulted in a reduction in the normal stress on the joint plane which reduces the frictional resistance of the joint to become mainly cohesive with a significant reduction in the frictional resistance. Pillars could be subjected to a fatigue failure because of floor benching since they experience a cycle of loading-unloading-reloading. The loading cycle occurred for the perimeter pillars. The unloading cycle occurred for partly benched and fully benched pillars. As floor benching continues, the pillars will be loaded back to their tributary load. Floor benching, karst cavities and geological discontinuities can trigger large uncontrolled displacement and shear failure along joint planes because of changing the joint condition from being constrained to being unconstrained. Also, they can induce high tensile stresses that can open joints and accelerate weathering. Therefore, it is recommended to consult a geotechnical engineer if the quality of the rock mass is poor due to karst features and geological discontinuities and floor benching will be conducted.

LIMITATION OF THE STUDY

The work completed in this study was to gain more insight about three factors associated with a massive pillar failure occurred in an underground limestone mine using numerical models. These factors are floor benching, geological discontinuities, and karst cavities. The model results and the conclusions drawn from this study depend on the input parameters and the boundary conditions used in the simulation. For example, the presumed joint condition, joint spacing, joint dip, and the shape and dimension of the karst cavity reflect the conditions observed near the collapsed area at the study mine. These variables may vary from mine to mine. Additionally, the model inputs, such as the seam inclination, depth of cover, and extraction ratio could be different from what were used in this study. Therefore, the results and conclusions drawn from this study may or may not be completely applicable to other mines.

DISCLAIMER

The findings and conclusions in this study are those of the authors and do not necessarily represent the official position of

the National Institute for Occupational Safety and Health (NIOSH), Centers for Disease Control and Prevention (CDC). Mention of any company or product does not constitute endorsement by NIOSH.

REFERENCES

1. Baggett, J., Abbasi, A., Monsalve, J. et al. (2020). “Ground-Penetrating Radar for Karst Detection in Underground Stone Mines.” Mining, Metallurgy & Exploration 37, 153–165. https://doi.org/10.1007/s42461-019-00144-1.

2. Bandis, S.C., Lumsden, A.C., and Barton, N.R. (1983). “Fundamentals of rock joint deformation.” Int. J. Rock Mech. Min. Sci & Geomech. Vol. 20. No. 6. Printed in Great Britain. Pp. 249-268.

3. Barton, N. (1976). “Rock mechanics review, the shear strength of rock and rock joints.” Int J. Rock Mech. Min. Sci & Geomech. Vol 13, Pergamon Press. Printed in Great Britain. Pp. 255-279.

4. Boyd, J.M. (1975). “The interpretation of geological structure for engineering design in rock” Ph.D thesis submitted to the university of London. Imperial college of science and technology.

5. Brady, B.H.G. and Brown, E.T. (2004). “Rock mechanics for underground mining.” Third Edition, Kluwer Academic Publishers.

6. Esterhuizen G, Tyrna P, and Murphy MM (2018). “A Case Study of Pillar Collapse at a Limestone Mine in Pennsylvania.” Proceedings of the 52nd US Rock Mechanics/Geomechanics Symposium, ARMA 18-363, Seattle, WA, 17 – 20 July 2018, 8 p.

7. Esterhuizen, G.S., Dolinar, D.R., and Ellenberger, J.L. (2008). “Pillar strength and design methodology for stone mines.” In: Proceedings of the 27th International Conference on Ground Control in Mining. Morgantown, WV: West Virginia University, pp. 241–253.

8. Esterhuizen, G.S., Dolinar, D.R., and J.L. Ellenberger. (2007). "Observations And Evaluation of Floor Benching Effects On Pillar Stability In U.S. Limestone Mines." Paper presented at the 1st Canada - U.S. Rock Mechanics Symposium, Vancouver, Canada, May 2007.

9. Esterhuizen, G.S., Dolinar, D.R., Ellenberger, J.L., and Prosser, L.J. (2011). “Pillar and roof span design guidelines for underground stone mines.” Pittsburgh, PA: NIOSH IC9526, pp. 1–64.

10. Evanek, N., Iannacchione, A., Anderson, T. (2022). “A Case Study of Potential Geologic Factors Affecting the Occurrence of Massive Strata Collapses in an Underground Limestone Mine in Southwestern Pennsylvania.” 41st International Conference on Ground Control in Mining, Canonsburg, PA, July 26-28, 2022.

11. Goodman, R., (1989). “Introduction to rock mechanics.” Second Edition. John Wiley & Sons.

12. Hoek E, Brown ET. (1980). “ Underground excavations in rock.” London: The Institution of Mining and Metallurgy.

13. Hoek, E., and Diederichs, M.S. (2006). “Empirical estimation of rock mass modulus.” International Journal of Rock Mechanics and Mining sciences. Vol. 43, Issue 2, pp. 203–2015.

14. Hoek, E., Kaiser, P.K. and Bawden, W.F. (1995). “Support of Underground Excavation in Hard Rock.” Balkema, Rotterdam.

15. Iannacchione A., Esterhuizen G., and Tadolini S. (2007). “Using Major Hazard Risk Assessment to Appraise and Manage Escapeway Instabilities Issues: A Case Study”, Proceedings in the 26th International Conference on Ground Control in Mining, Morgantown, WV, 31 July – 2 August, pp. 354-360.

16. Itasca Consulting Group, Inc. (2019). UDEC — Universal Distinct Element Code, Ver. 7.0. Minneapolis: Itasca.

17. Itasca Consulting Group, Inc. (2020). “Griddle, Ver. 2.0.” Minneapolis: Itasca.

18. Jaeger, J. C. (1960). “Shear fracture of anisotropic rocks.” Geol. Mag., 97. Pp. 65–72.

19. Martin, C.D. and Maybee, W.G. (2000). “The strength of hard rock pillars.” International Journal of Rock Mechanics and Mining Sciences, vol. 37. pp. 1239–1246.

20. McNeel, R. et al. (2010). Rhinoceros 3D, Version 6.0. Robert McNeel & Associates, Seattle, WA.

21. Phillipson, S., (2012). “Massive Pillar Collapse: A Room-and-Pillar Marble Mine Case Study.” Proceedings of the 31st International Conference on Ground Control in Mining, Morgantown, WV: West Virginia University, 9 P.

22. Rashed, G., Evanek, N., Van Dyke, M., Mazella, M., and Slaker, B. (2023). “A Study of the Leading Factors Associated with a Massive Ground Collapse in an Underground Limestone Mine in Southwestern Pennsylvania.” 42nd International Conference on Ground Control in Mining, Canonsburg, PA, July 26-28.

23. Rumbaugh G.M., Mark, C., Kostecki, T. (2022). “Massive Pillar Collapses in U.S. Underground Limestone Mines: 2015-2021.” 41st International Conference on Ground Control in Mining, Canonsburg, PA, July 26-28, 2022